

Annex 6

Effect of emulsification conditions on mean drop-size.

Ivan. B. Ivanov¹, Nina Vankova,¹ Slavka Tcholakova,¹ Vasko Vulchev¹
and Nikolai D. Denkov¹

*¹Laboratory of Chemical Physics & Engineering,
Faculty of Chemistry, Sofia University, 1164 Sofia, Bulgaria*

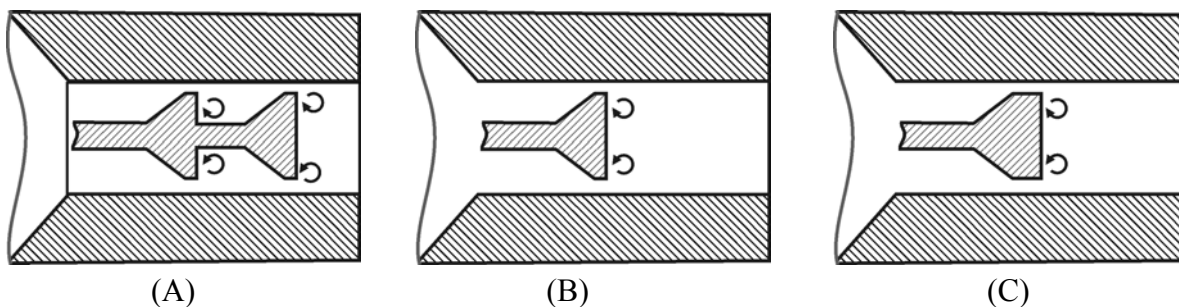
ABSTRACT

In this part of the Report we describe experimental results obtained with narrow-gap homogenizer of cylindrical geometry. The effects of: (1) Construction of the processing element; (2) Viscosity of the aqueous phase; and (3) Viscosity of the oil phase on the mean drop size are studied. All experiments are performed in excess of emulsifier and the effect of drop-drop coalescence is negligible during the emulsification.

The role of the construction of the processing element was studied by comparing three different constructions. We found that the construction of the processing element affects slightly the flow rate of the emulsion through the homogenizer, at fixed driving pressure and gap width, which indicates that the construction of the element does not affect tremendously the hydrodynamic conditions. Furthermore, we found that the mean drop size of the emulsions made with different elements agrees with the prediction of Kolmogorov-Hinze equation, under the assumption that the volume, in which the energy dissipation takes place, is approximately the same for all studied elements.

The role of oil viscosity was studied with silicone oils having viscosity between 50 and 1000 mPa.s. The emulsification of silicone oils with viscosity below 600 mPa.s was successful (micrometer sized drops were obtained), whereas the silicone oils with higher viscosity could not be entirely dispersed into small drops (millimeter sized drops were observed in the final emulsion). This experimental fact is explained by comparing the drop residence time with the drop deformation time in the processing element. For successful emulsification, the residence time should be around 10 times longer than the deformation time.

The role of the viscosity of aqueous phase is studied by adding thickening agent (glycerol). The increased viscosity of the aqueous phase leads to changing the regime of emulsification from inertial turbulent to viscous turbulent. The experimental results for the mean drop size in emulsions produced in viscous turbulent flow are fitted with appropriate equation. The volumes, in which the main dissipation of turbulent energy takes place, were found to be similar for emulsification in inertial viscous and inertial turbulent regimes.



Schematic presentation of the used processing elements with gap-width of 395 μm : (A) Element with two cones, GW395-2C; (B) Element with single cone, GW395-1C; (C) Element with single cone of double length, GW395-1CDL.

1. Aim of the study.

One of the aims of the experiments, described in this part of the Report, is to test the new custom-made emulsification device, which enables emulsification at various driving pressures, without using a pump (the latter could break the droplets, affecting in this way the results from the emulsification experiments). More important, the performed experiments have given us the possibility to make a comparative estimate of the importance of various factors in the emulsification process. We carried out three series of experiments, aimed to clarify the effects of: (1) construction of the processing element, (2) viscosity of the dispersed phase, and (3) viscosity of the continuous phase, on the mean drop size, d_{32} , of the obtained emulsions.

2. Materials and methods.

2.1. Materials.

We used two types of emulsifier, at high concentrations, to prepare stable oil-in-water emulsions. As a protein emulsifier we used whey protein concentrate (WPC, trade name AMP 8000; product of Proliant), and as a low-molecular mass surfactant – the nonionic polyoxyethylene-8 tridecyl ether (ROX, product of Rhodia). Both emulsifiers were used as received. All aqueous solutions were prepared with deionized water, purified by a Milli-Q Organex system (Millipore). The protein solutions, along with WPC, contained inorganic electrolyte NaCl (Merck, analytical grade) with concentration of 150 mM and 0.01 wt % of the antibacterial agent NaN_3 (Riedel-de Haën).

As dispersed phase we used three types of oil, which differ in their chemical composition and viscosity: soybean oil (SBO, commercial product) with viscosity of 50 mPa.s; hexadecane (product of Merck) with viscosity of 3.13 mPa.s (at $T = 28^\circ\text{C}$) and silicone oils SH200C (product of TDCS), Rhodorsil 621V600 and 47V1000SH (products of Rhodia), with viscosities of 50, 600, and 1000 mPa.s, respectively. The oils were used as received.

For varying the viscosity of the continuous phase we added thickening agents in the surfactant solutions. We used glycerin (99.5 %, p.a.) or sugar (commercial product) of various weight concentrations.

The viscosity of the hexadecane, and of the surfactant and glycerin solutions was measured by means of a capillary-type viscometer. The viscosity of SBO, silicone oils, and protein solutions containing sugar was measured by a Brookfield Rheoset viscometer, see Chapter 1, section 1.2.5.

2.2. Construction of the homogenization chamber.

All emulsions were prepared by using custom-made equipment, called “narrow-gap homogenizer”. It has a modified construction in comparison with the homogenizer, which had been used so far (see [1-2]). Like the previous experimental set-up, the new one consists of pipes, a turn-cock, and a mixing head with cylindrical geometry. The mixing head is equipped with a processing element, containing narrow slits, which may have different widths and lengths. These narrow slits promote a high density of turbulent power dissipation, locally inside the slits and in the regions just after them. In these regions of high rate of energy dissipation, the deformation and breakup of the emulsion drops takes place. Four different processing elements were used in our experiments. Three of them ensure gap-width of 395 μm in the emulsification chamber and the forth one – gap-width of 485 μm . The three elements with 395 μm gap-width differ in their construction, as shown in Figure 1.

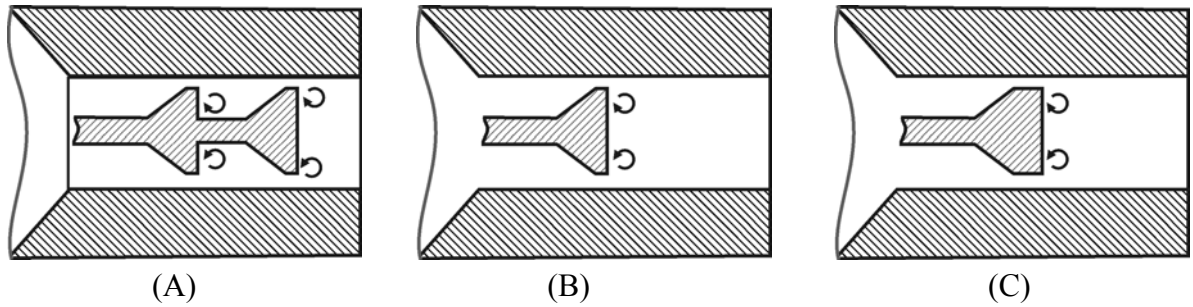


Figure 1. Schematic presentation of the used processing elements with gap-width of 395 μm : (A) Element with two cones, GW395-2C; (B) Element with single cone, GW395-1C; (C) Element with single cone of double length, GW395-1CDL.

It is seen from Figure 1 that each processing element includes one or two small bodies (sub-elements) with a conic shape. Each of these sub-elements has an outer “working” surface, parallel to the wall of the pipe, which is involved in the formation of the narrow gap.

The processing element, shown in Figure 1A, consists of two consecutively connected cones, each of them with 1 mm length of the working surface. The construction of the element with gap-width of 485 μm is the same. Element (B) consists of a single cone with the same length of the working surface, 1 mm. Element (C) also consists of a single cone, but the length of the working surface is 2 mm. For brevity, we use the following abbreviations for these processing elements: GW395-2C for element (A); GW395-1C for element (B) and GW395-1CDL for element (C). In this notation GWXXX indicates the gap-width of the element, 1C or 2C shows the number of consecutively connected cones, and DL indicates the doubled length (2 mm) of the narrow gap in the respective cone.

Besides the construction of the processing element, we can modify the configuration of the emulsification head after the element, by changing the width and the length of the outgoing pipes. In a single experiment we put a Teflon insertion inside the pipe, immediately after the processing element GW395-2C, in order to create a narrower orifice of the outgoing pipe. This modification is marked in the text as GW395-2C_{ins} (Ins = insertion). In another experiment we increased the distance between the homogenization chamber and the outlet of the equipment by attaching an additional pipe after the element GW395-2C. This modification is denoted as GW395-2C_{Ext} (Ext = extension).

In contrast to the previous homogenizer, the new one (Figure 2) is constructed without a pump to eliminate the possibility for drop breakage outside the mixing head. Additionally, the new construction allows one to vary the pressure at the inlet of the emulsification chamber for a given processing element (this was impossible with the previous equipment). Therefore, the new equipment gives us the opportunity to study separately several important factors – applied pressure, shape of the processing element, gap-width of the slits, and to evaluate the role of each of these factors for the emulsification process.

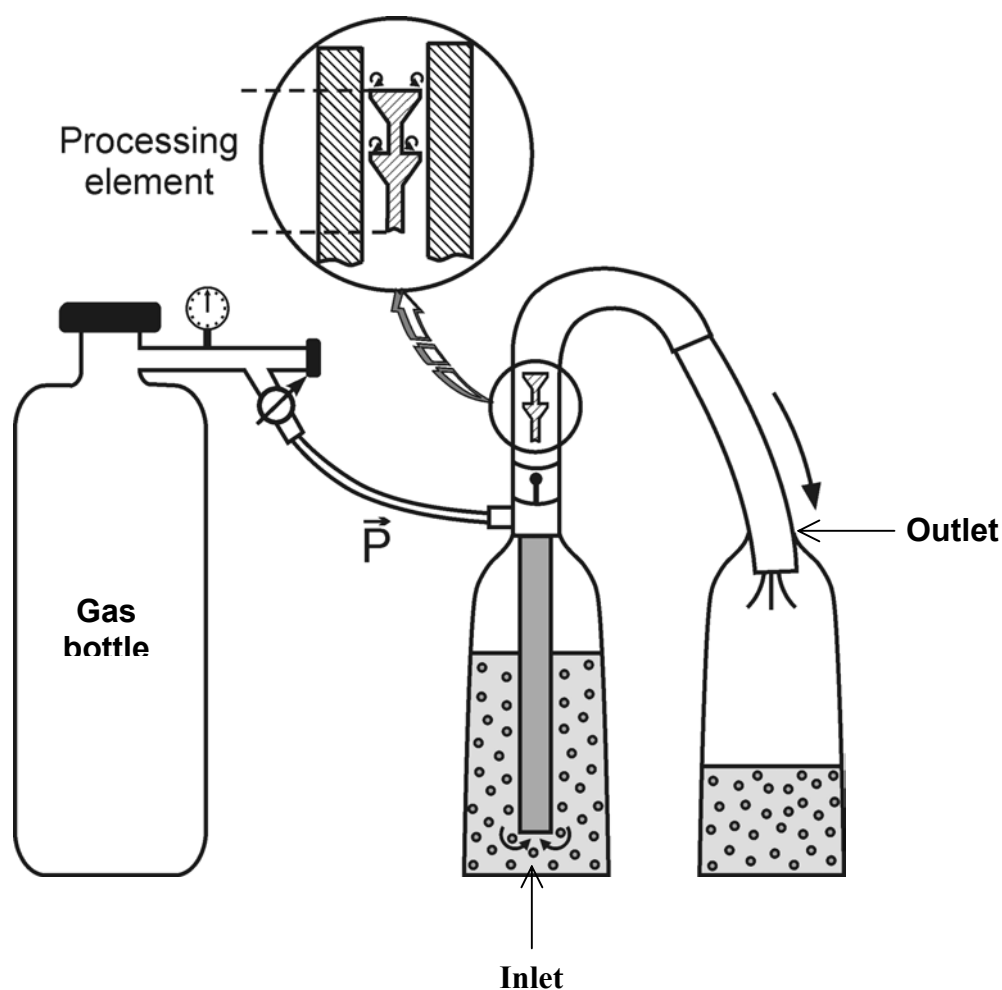


Figure 2. A schematic presentation of the modified narrow-gap homogenizer used for emulsion preparation.

In the new construction, the driving pressure for passing the oil-water mixture through the emulsification element is provided by a gas N₂-bottle. The latter is connected by means of a Tygon hose to the fitting element between the vessel and the ingoing pipe for the emulsion, on one side, and to the turn-cock on the other side, see Figure 2.

The construction of the modified homogenizer does not allow one to perform a continuous circulation of the mixture in a closed loop (this mode of emulsification was realized in the previous set-up). The new apparatus enables emulsification only in a discontinuous mode: after each pass of the oil-water mixture through the homogenization element, the process is stopped for bringing the obtained emulsion back into the inlet of the device. The exact emulsification procedure is described in the following subsection.

2.3. Procedure for emulsion preparation.

Oil-in water emulsions were prepared by using a two-step procedure. Initially, an oil-in-water premix was prepared by hand-shaking a vessel, containing the necessary amounts of oil and surfactant solution (depending on the desired oil volume fraction in the final emulsion). The total volume of the emulsions in the performed experiments was 700 mL. The second homogenization step was accomplished by passing this premix through the homogenizer. The desired pressure was ensured by the gas bottle and was applied directly upon the premix in the vessel, at the inlet of the apparatus. After passing through the ingoing pipe and the narrow slits in the mixing head, the oil-water mixture was collected in the vessel at the outlet. Then the gas flow was stopped for a while, the vessel with the emulsion was moved from the outlet to the inlet of the device, and the process was repeated to accomplish the next pass of the mixture through the emulsification head. In each experiment, this procedure was repeated 10 times, which corresponds to 10 passes of the used oil-water mixture through the homogenizer. The driving pressure was varied in the range between 0.5×10^5 and 3×10^5 Pa. The experimental error of the pressure measurements in the preliminary experiments was $\pm 0.15 \times 10^5$ Pa.

In all experiments, a pair of plastic bottles of equal shape, size and volume was used for collecting the emulsion during the homogenization process.

Experimental results, obtained with the previous equipment, had shown that the stationary state of the drop-size distribution is reached after at least 50 cycles (passes) of the oil-water mixture through the processing element (see [1-2]). Hence, the duration of the emulsification procedure for the experiments, described in this chapter of the Report (10 passes), was insufficient for reaching the steady-state distribution. This circumstance was taken into account in the interpretation of the experimental results and when formulating the conclusions.

The drop size distribution of the studied emulsions was determined by optical microscopy, as described in section 1.2.4 of Chapter 1.

3. Experimental results and discussion.

The current section is organized as follows: Section 3.1 describes results about the effect of hydrodynamic conditions (construction of the homogenization head) on the mean drop size, d_{32} . In section 3.2, the effect of the viscosity of dispersed (oil) phase on d_{32} is studied and discussed. In section 3.3 we present and discuss experimental results for the dependence of d_{32} on the viscosity of the continuous (aqueous) phase.

All emulsions, studied in this Report, were prepared in excess of emulsifier (surfactant). According to previous studies [1-2], a significant steric and/or electrostatic repulsion arises in such systems and suppresses the drop-drop coalescence. Therefore, the mean drop-size in this part of the study is determined exclusively by the process of drop breakup. The experiments, described in this chapter, were planned as preliminary tests of the new homogenizer. For that reason, as already mentioned in section 2.3, the steady-state drop-size distribution was not reached. Hence, the obtained results should be considered mainly as comparative for the various conditions and systems studied.

3.1. Effect of hydrodynamic conditions on the mean drop size.

The hydrodynamic conditions during emulsification are characterized by the power density of energy dissipation, ε , in the mixing chamber of the homogenizer. It was shown [1-2] that in turbulent flow, at high emulsifier concentrations (so-called “surfactant-rich” regime [3]), the energy dissipation rate plays a decisive role for the mean size of the emulsion droplets. In this regime, the type of the used emulsifier affects the mean drop-size mainly through the equilibrium value of the oil-water interfacial tension, σ_{OW} . The coalescence rate is negligible under these conditions and, according to the Kolmogorov-Hinze theory of emulsification in turbulent inertial regime [4-5], the mean drop diameter, d_{32} , can be estimated by comparing the fluctuations of the hydrodynamic pressure in the flow with the capillary pressure of the drops. The respective equation for the mean drop-size reads:

$$d \approx \varepsilon^{-0.4} \sigma_{OW}^{0.6} \rho_C^{-0.2} \quad (1)$$

where ρ_C is the mass density of the continuous phase.

The power density of energy dissipation can be found from the relation:

$$\varepsilon = \frac{pQ}{V_{DISS}} \quad (2)$$

where p is the pressure difference between the inlet and the outlet of the emulsification element, Q is the flow rate, and V_{DISS} is the volume of the mixing chamber, where the turbulent dissipation of energy takes place.

In the experiments, described in the current section, we varied the value of ε by changing the applied pressure, the construction of the used processing element, and the gap-width of the slits in the element. The experiments were performed at two different pressures: 0.98×10^5 Pa and 2.16×10^5 Pa. Four different processing elements, GW395-2C, GW395-1C, GW395-1CDL and GW485-2C, see Figure 1, were tested. Experiments with changed configuration of the mixing chamber after the processing element (denoted as GW395-2C*Ins* and GW395-2C*Ext*) were also performed (see section 2.1).

Oil-in-water emulsions were prepared by using the procedure, described in section 3.2 of Annex 5. The emulsions contained soybean oil with fixed oil volume fraction ($\Phi = 0.28$), and solution of WPC + 150 mM NaCl as an aqueous phase. WPC was with concentration of 1 or 3 wt %. The experimental results for d_{32} , obtained in this series of experiments, are presented in Table 1.

Table 1. Mean volume-surface diameter, d_{32} , at two driving pressures and different processing elements, at two WPC concentrations. All solutions contain 150 mM NaCl and 0.01 wt. % NaN₃. The oil phase is SBO with $\Phi = 0.28$.

Processing element	d_{32} , μm (10 passes)			
	1 wt % WPC		3 wt % WPC	
	$p = 0.98 \times 10^5$, Pa	$p = 2.16 \times 10^5$, Pa	$p = 0.98 \times 10^5$, Pa	$p = 2.16 \times 10^5$, Pa
GW395-2C	20.2	13.8	19.6	11.1
GW395-1C	18.7	12.3	14.8	10.1
GW395-1CDL	17.2	12.2	—	—
GW395-2C <i>Ins</i>	—	—	16.8	10.4
GW395-2C <i>Ext</i>	—	—	—	9.0
GW485-2C	—	—	17.0	—

It is seen that, as predicted by Kolmogorov-Hinze theory, eq 1, the increase of the applied pressure, viz. the increase of ε , eq 2, leads to a significant decrease of the mean drop-size in a given system, for each of the used processing elements.

The experiments, performed at a given pressure, show that d_{32} changes when using different processing elements, or when modifying the construction immediately after the element. The different processing elements may alter the values of Q and/or V_{DISS} , thus changing ε , at a fixed pressure. In our experiments, we measured the flow rate and found

it to vary no more than 20 %, when using the various processing elements. There is no way to measure exactly the dissipation volume, since the latter is not equivalent to the geometrical volume of the narrow slits, V_S (for more details see Ref. 1).

To see the trends in the change of the mean drop-size when using different elements, at a given pressure, we compared the experimental values of d_{32} with the values of the Kolmogorov-Hinze diameter, d_K , predicted by eq 1. To calculate d_K we assume that V_{DISS} remains unchanged for the different processing elements with GW 395 μm . We used $V_{DISS} \approx 1.72 \times 10^{-7} \text{ m}^3$, as estimated in our previous study, see Refs. 1-2. The other parameters used in these estimates are $\sigma_{OW} = 10 \text{ mN/m}$ (experimentally measured value for the WPC solutions used) and $\rho_C = 10^3 \text{ kg/m}^3$. The obtained values for the ratio d_{32}/d_K are presented in Table 2.

Table 2 Values for d_{32}/d_K , calculated for different processing elements (GW 395), at two driving pressures and two WPC concentrations. d_K is calculated according to eq 1, assuming a constant dissipation volume, $V_{DISS} = 1.72 \times 10^{-7} \text{ m}^3$. The other parameters used in these calculations are $\sigma_{OW} = 10 \text{ mN/m}$ and $\rho_C = 10^3 \text{ kg/m}^3$.

Processing element	d_{32}/d_K			
	1 wt % WPC		3 wt % WPC	
	$p = 0.98 \times 10^5$, Pa	$p = 2.16 \times 10^5$, Pa	$p = 0.98 \times 10^5$, Pa	$p = 2.16 \times 10^5$, Pa
GW395-2C	1.5	1.7	1.6	1.4
GW395-1C	1.6	1.6	1.4	1.4
GW395-1CDL	1.5	1.6	—	—
GW395-2C _{Ins}	—	—	1.3	1.3
GW395-2C _{Ext}	—	—	—	1.1

As seen from Table 2, the ratio d_{32}/d_K is equal to 1.5 ± 0.1 for the three processing elements with GW395, despite the specific construction of the element (see the first three rows in the table). This result was obtained at both WPC concentrations and both applied pressures. The observed slight variations in d_{32}/d_K do not follow any obvious trend and fall in the range of the experimental error of measuring p and Q . Hence, we may conclude that the assumption that V_{DISS} remains constant is acceptable for the processing elements with modified construction (GW395-2C, GW395-1C and GW395-1CDL). In other words, modifications in the construction of the processing element, like those shown in Figure 1, do not lead to a significant change of the volume of energy dissipation.

The observed higher value of d_{32} in comparison with the theoretically predicted d_K , can be explained by the fact that the studied emulsions are passed only 10 times

through the processing element, without reaching the steady-state value of the mean drop-size. This explanation was confirmed by the systematic set of experiments, described in Chapter 1 of this Report. Just as an example, in one of the experiments performed at $p = 0.98 \times 10^5$ Pa and GW395-2C with 1 wt % Brij 58 (150 mM NaCl) + SBO, the ratio d_{32}/d_K was 1.7, when using the value of d_{32} , measured after the 10th pass through the homogenizer (see Annex 4, Figure 1). The mean drop-size further decreases with the number of passes leading to a ratio $d_{32}/d_K \approx 0.8$ after the 100th pass.

The situation seems different in the cases when we keep the processing element unchanged and modify the construction after it, by altering the width or the length of the outgoing pipe (see the last two lines in Table 2). Here we obtain lower values for the ratio d_{32}/d_K , which indicates that the assumption for a constant dissipation volume is not valid. These results indicate that the dissipation volume of the modified processing elements is smaller, as compared to the original processing element GW395-2C. Optical observations by a high-speed camera and/or numerical simulations of the turbulent flow in the various processing elements could be very useful to understand and analyze the observed effects.

In conclusion, the experimental results for the effect of the various hydrodynamic conditions on the mean drop-size can be described by the theory of emulsification in turbulent inertial regime. More detailed experimental and theoretical studies would be useful to determine more accurately the dissipation volume in the emulsification chamber.

3.2. Effect of the viscosity of the dispersed (oil) phase.

3.2.1. Effect on the mean drop-size.

The effect of oil viscosity, η_D , on the mean drop-size was studied with ROX-stabilized emulsions, prepared with silicone oils having viscosities 50, 600 and 1000 mPa.s. For complete suppression of the drop-drop coalescence, the emulsifier concentration was fixed at 5 wt % and the oil volume fraction was relatively low, $\Phi = 0.1$. Experiments at three different driving pressures, 0.49×10^5 , 0.98×10^5 and 2.16×10^5 Pa, were performed, by using the processing element GW395-2C. The obtained results for d_{32} are shown in Table 3.

Table 3. Mean volume-surface diameter, d_{32} , for three silicone oils with different viscosities, at three different driving pressures. The aqueous phase is 5 wt % ROX, the oil volume fraction $\Phi = 0.1$, and the processing element is GW395-2C.

η_D , mPa.s	d_{32} , μm		
	$p = 0.49 \times 10^5$, Pa	$p = 0.98 \times 10^5$, Pa	$p = 2.16 \times 10^5$, Pa
50	6.9	6.2	5.6
600	100 μm drops	50 μm drops	7.6
1000	millimeter sized drops	millimeter sized drops	millimeter sized drops

These results show that the silicone oil with viscosity of 50 mPa.s is the only one, which is successfully emulsified under all driving pressures applied. We obtained stable emulsions of this oil and, as predicted from the theory, the mean drop-size decreased with the increase of the applied pressure.

With the silicone oil of 600 mPa.s we managed to prepare a stable emulsion only at the highest driving pressure, $p = 2.16 \times 10^5$ Pa (i.e., at the highest value of ε). At lower pressure we obtained rather polydisperse emulsions with relatively large fraction of drops, whose diameters fell in the range between 50 and 100 μm .

We failed to obtain fine emulsion of silicone oil with $\eta_D = 1000$ mPa.s. The obtained emulsions contained millimeter sized drops, of high concentration, which quickly moved upwards due to buoyancy force and coalesced at the emulsion surface.

From these results we can conclude that there is a threshold value of the oil viscosity, above which the emulsification is very inefficient. To check the exact value of this “threshold” oil viscosity, we will perform experiments with silicone oils having viscosity in the range between 50 and 600 mPa.s.

3.2.2. Deformation time vs. residence time – a possible criterion for emulsification efficiency.

In systems with suppressed coalescence (like those studied in the present chapter of the Report) poor emulsification means that the process of drop breakage is inefficient. It is known from literature [2, 6-7] that one of the main parameters, which determines the rate of drop breakup in turbulent flow, is the so called “deformation time”, τ_{DEF} . This is the time needed for deforming the drops to a sufficiently large aspect ratio, so that Rayleigh type of capillary instability could occur. For viscous drops, the deformation time can be calculated from the expression (see Ref. 7-8):

$$\tau_{DEF} \approx \frac{\eta_D}{\varepsilon^{2/3} d^{2/3} \rho_C^{1/3}} \quad (3)$$

Equation 3 predicts that τ_{DEF} increases with the viscosity of the dispersed phase and decreases with the drop diameter, d . For the used silicone oils, we calculated τ_{DEF} for drops with diameters of 5, 10, 20, 30 and 50 μm , at the three pressures applied (see Figure 1).

Since the drop deformation and breakage occur exclusively in the processing element (due to the much higher density of energy dissipation there), we should compare τ_{DEF} with the average residence time, t_R , of the droplets in the mixing chamber, in order to estimate the efficiency of the emulsification process. The drops should have sufficient time for deformation and breakup, while traveling along the processing element, and hence, the deformation time should be shorter than the residence time. The latter can be found from the relation V_{DISS}/Q , taking into account that $V_{DISS} \approx 1.72 \times 10^{-7} \text{ m}^3$ in our equipment and that the flow rate, Q , is different for the different pressures. We calculated the following values for the residence times: $t_R \approx 2.8 \text{ ms}$ at $p = 0.49 \times 10^5 \text{ Pa}$, $t_R \approx 1.9 \text{ ms}$ at $p = 0.98 \times 10^5 \text{ Pa}$, and $t_R \approx 1.3 \text{ ms}$ at $p = 2.16 \times 10^5 \text{ Pa}$.

For comparison, in Figure 1 we present the dependence of τ_{DEF} on drop diameter for the used silicone oils, as well as the estimated value of t_R for the respective working pressure, see Figure 3. The comparison of the theoretical estimates (Figure 3) and of the experimental results (Table 3) shows that, for successful deformation and breakup of 30-50 μm sized drops, the deformation time should be at least 1 order of magnitude shorter than the residence time. When the difference between τ_{DEF} and t_R is smaller, as it is for oils with viscosities of 600 (at the lower driving pressure) and 1000 mPa.s, the breakage of the drops is suppressed, which leads to inefficient emulsification, even in excess of emulsifier and at low oil volume fraction. Note that the breakage rate constant rapidly decreases with the increase of oil viscosity, as shown in Annex 4.

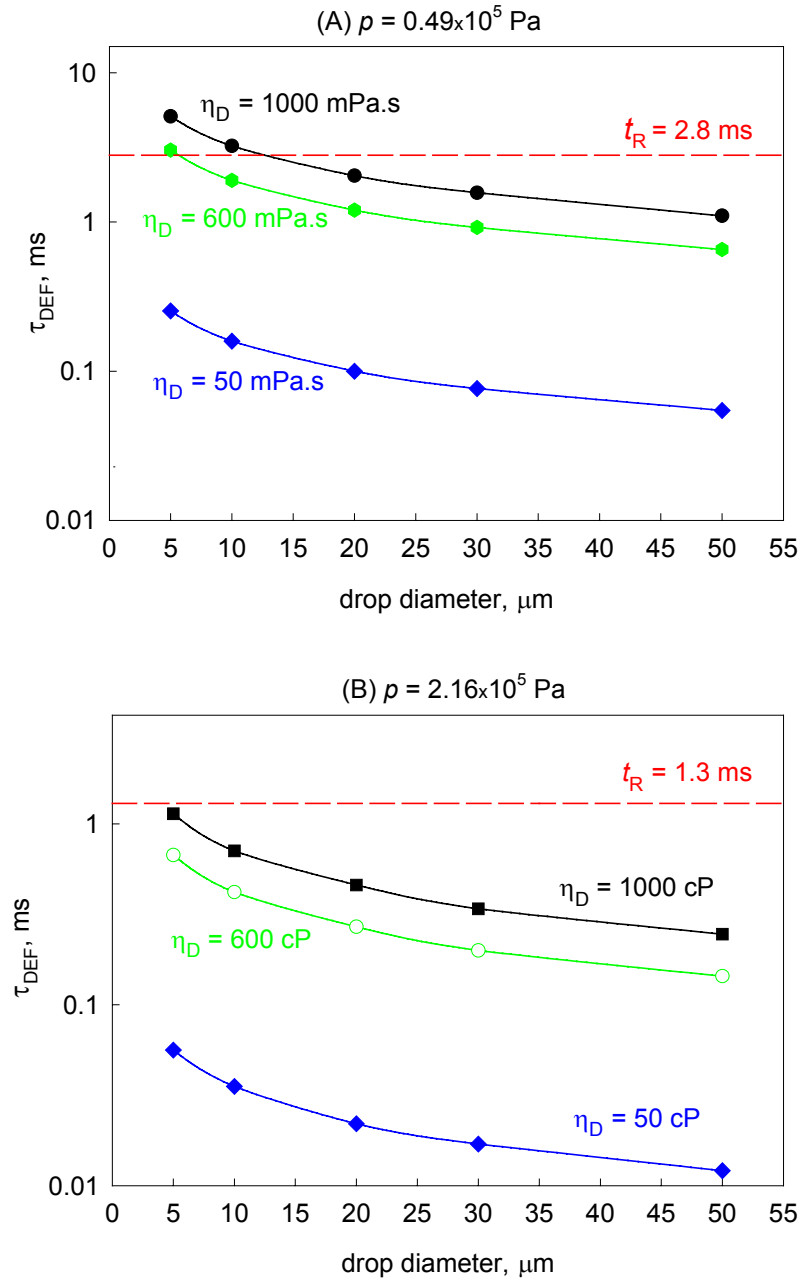


Figure 3. Calculated values for $\tau_{DEF}(d)$, for the used silicone oils and the value of t_R for: (A) $p = 0.49 \times 10^5$ Pa and (B) $p = 2.16 \times 10^5$ Pa.

3.3. Effect of the viscosity of the continuous (aqueous) phase.

The viscosity of the continuous phase, η_C , may affect both the processes of drop breakage and drop-drop coalescence. According to Kolmogorov's theory, η_C is one of the factors, which determine the size, λ_0 , of the smallest turbulent eddies in the continuous phase [4-5,9]:

$$\lambda_0 \sim \varepsilon^{-0.25} \eta_C^{0.75} \rho_C^{-0.5} \quad (4)$$

If the produced drops are larger in diameter than the smallest turbulent eddies ($d > \lambda_0$), the drop breakup is controlled by inertial hydrodynamic forces and the emulsification occurs in the so-called “turbulent inertial” regime. In this regime, the mean drop-size depends slightly on the viscosity of the continuous phase and could be estimated by eq 1.

On the other hand, if $d < \lambda_0$, drop breakage is governed by the shear (viscous) stresses inside the smallest eddies of the turbulent flow [4-5,8,10]. This is the so-called “turbulent viscous” regime of emulsification, in which the mean drop diameter could be calculated by using the following relation [8]:

$$d \approx \varepsilon^{-0.5} \sigma_{ow} \eta_C^{-0.5} \quad (5)$$

As seen from eq 5, the mean drop size in turbulent viscous regime depends not only on the average power density, interfacial tension and mass density of the continuous phase, but also on the viscosity of the continuous phase - d decreases with the increase of η_C . Let us remind that eqs 1 and 5 were derived under the assumption that drop breakage is predominant during the emulsification process and the coalescence between the droplets can be neglected.

We studied the role of η_C by preparing emulsions in the “surfactant-rich” regime, in which the drop-drop coalescence is negligible and the mean drop-size is determined exclusively by the drop breakage process. We performed two types of experiments by preparing oil-in-water emulsions with: 1) *lower viscosity of the aqueous phase* in comparison with the oil viscosity, and 2) *higher viscosity of the aqueous phase* in comparison with the oil viscosity. For each of the two experimental series, the oil viscosity was kept constant, while the viscosity of the continuous phase was varied by addition of thickening agents in the aqueous phase. In the following subsections we present and discuss the obtained results.

3.3.1. Lower viscosity of the aqueous phase in comparison with the oil viscosity.

Two series of experiments were performed with SBO-in-water emulsions, all of them with oil viscosity $\eta_D = 50$ mPa.s and volume fraction $\Phi = 0.28$. These emulsions were stabilized by 5 wt % ROX and the viscosity of the aqueous phase for one of these emulsions was increased by addition of 50 wt % glycerin. Thus we managed to raise η_C up to 13 mPa.s, respectively. Emulsification at three different driving pressures, 0.49×10^5 , 0.98×10^5 , and 2.16×10^5 Pa, with the processing element GW395-2C was performed. The obtained experimental results for the mean drop size are shown in Table 4.

Table 4. Mean volume-surface diameter, d_{32} , for 5 wt % ROX-stabilized emulsions with different aqueous viscosity (varied by addition of glycerin). The oil phase is SBO ($\Phi = 0.28$; $\eta_D = 50$ mPa.s). The emulsification is performed at three different pressures, with processing element GW395-2C.

Experimental system	η_C , mPa.s	$p = 0.49 \times 10^5$, Pa		$p = 0.98 \times 10^5$, Pa		$p = 2.16 \times 10^5$, Pa	
		d_{32} , μm	λ_0 , μm	d_{32} , μm	λ_0 , μm	d_{32} , μm	λ_0 , μm
5 wt % ROX	1.9	not measured		4.6	3.3	3.97	2.5
5 wt % ROX 50 wt % glycerin	13.0	3.9	18.7	3.4	14.6	2.6	11.1

When comparing the emulsions with and without glycerin, prepared at a given pressure (0.98×10^5 or 2.16×10^5 Pa), one sees that the values of d_{32} are smaller at higher viscosity of the aqueous phase. An estimate of the size of the smallest eddies, λ_0 , shows that it is comparable to the mean drop-size d_{32} , in the system without glycerol. As shown in ref 2, d_{32} in this case is proportional to λ_0 and cannot be estimated by eq 1. Indeed, the ratio d_{32}/λ_0 for these emulsions is equal to 1.5 ± 0.1 . On the other hand, for the system with high viscosity of the aqueous phase (50 wt % glycerol) the mean drop-size is much smaller than λ_0 , which shows that the emulsification occurs in the viscous turbulent regime for this system. As expected, the experimental values for d_{32} are close (within 30 %) to those calculated by eq 5 ($\sigma_{OW} \approx 2.5$ mN/m, measured for this system, was used in the calculations). More precise comparison of the theoretical and experimental data is not justified for this system, at the present moment, because the experimental data do not correspond to a steady-state drop size.

For accurate determination of the threshold value of η_C , at which a transition between the two different regimes of emulsification in turbulent flow occurs, emulsions with steady-state drop size distribution and precisely measured values of ε , σ_{OW} and ρ_C should be studied.

3.3.2. Higher viscosity of the aqueous phase in comparison with the oil viscosity.

The emulsions, described in this subsection, contained aqueous solution of 1 wt % WPC +150 mM NaCl + 60 wt % sugar as a continuous phase, and hexadecane with $\Phi = 0.1$ as an oil phase. The presence of 60 wt % sugar raised the aqueous viscosity up to 16.6 mPa.s, while the oil viscosity was 3.13 mPa.s. The emulsification was performed at five different driving pressures by using the processing element GW395-2C. The experimental results for d_{32} are presented in Table 5. As expected, the higher the applied pressure, the smaller mean size of the emulsion droplets was obtained.

To determine the type of emulsification regime for the studied emulsions, we calculated the size of the smallest turbulent eddies, λ_0 , according to eq 4. For this

calculation we took into account that $\eta_C = 16.6$ mPa.s, and $\sigma_{OW} \approx 10$ mN/m for all emulsions. Only the values of ε were different, since the applied pressures, p , and consequently the flow rates, Q , were varied. We assumed $V_{DISS} \approx 1.72 \times 10^{-7}$ m³, as estimated for the turbulent inertial regime, and calculated ε from eq 2. For comparison with d_{32} , the obtained values of λ_0 are also shown in Table 5.

Table 5. Experimentally obtained values of d_{32} and calculated values of λ_0 for 1 wt % WPC-stabilized emulsion, in presence of 60 wt % sugar ($\eta_C = 16.6$ mPa.s; $\rho_C = 1.2274$ g/cm³), with oil phase hexadecane with $\Phi = 0.1$ ($\eta_D = 3.13$ mPa.s). The solutions contain 150 mM NaCl and 0.01 wt. % NaN₃. The emulsification is performed at five different pressures, with processing element GW395-2C.

	$p = 0.49 \times 10^5$, Pa	$p = 0.98 \times 10^5$, Pa	$p = 2.06 \times 10^5$, Pa	$p = 2.16 \times 10^5$, Pa	$p = 3.14 \times 10^5$, Pa
d_{32} , μm	20.0	10.3	6.8	6.4	4.6
λ_0 , μm	21.6	16.9	12.9	12.7	10.6

It is seen that the mean drop diameter is smaller by about 6 micrometers than λ_0 for all emulsions, prepared at driving pressures equal to and above 0.98×10^5 Pa. Therefore, we may conclude that for the studied system, 1 wt % WPC + 60 wt % sugar + hexadecane (with $\Phi = 0.1$), the emulsification at $p \geq 0.98 \times 10^5$ Pa occurs in turbulent viscous regime. Hence, the mean drop diameter depends on the aqueous viscosity and could be estimated by eq 5.

The emulsion droplets, produced at $p = 0.49 \times 10^5$ Pa, are comparable in size with the smallest eddies, $d_{32} = 20$ μm vs. $\lambda_0 = 21.6$ μm . Most likely, this is the boundary case, when a transition from inertial to viscous regime of turbulent emulsification takes place.

One should note that when the emulsification regime changes, the volume of energy dissipation, V_{DISS} , could change as well. To check this possibility, we assumed that $d_{32} \approx d$ in eq 5, which predicts a linear dependence of the mean drop diameter on $\varepsilon^{-0.5}$, and plotted the obtained values of d_{32} as a function of $(pQ)^{-0.5}$. We fitted the experimental data with a linear equation, which turned out to describe well the experimental points, see Figure 4. From the slope of the theoretical fit we determined the volume of energy dissipation to be $V_{DISS} = 1.46 \times 10^{-7}$ m³ ($\eta_C = 16.6$ mPa.s and $\sigma_{OW} \approx 10$ mN/m were used in these calculations), which is in a good agreement with the dissipation volume estimated from the drop sizes, measured in turbulent inertial regime, $V_{DISS} = 1.72 \times 10^{-7}$ m³.

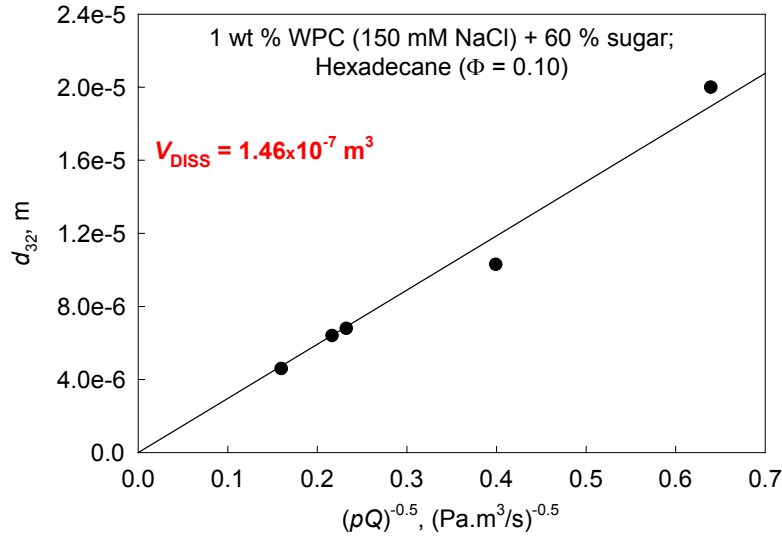


Figure 4. Mean volume-surface diameter, d_{32} , as a function of $(pQ)^{-0.5}$. The points are experimental values of d_{32} , whereas the line is a theoretical fit, according to eq 5. The parameters, used for calculation of V_{DISS} from the slope of the fit, are: $\eta_C = 16.6$ mPa.s and $\sigma_{OW} \approx 10$ mN/m.

4. Conclusions.

The effects of the construction of the processing element, viscosity of the oil phase, and viscosity of the continuous phase on the mean drop size during emulsification in turbulent flow were studied in excess of emulsifier. From the obtained experimental results we can conclude that:

- The presence of a second conical sub-element in the construction of the processing element does not affect significantly the hydrodynamic conditions and the emulsification efficiency. The flow rate is changed by around 20 % and the mean drop size decreases by around 10 %.
- The successful emulsification of oils with moderate viscosity, around 600 mPa.s, requires longer emulsification time and/or higher driving pressure. Most probably, the ineffective emulsification of oils with viscosity higher than 600 mPa.s is due to longer deformation time, high energy dissipated inside the drops, which results in lower rate of drop breakage.
- The increase of the viscosity of the aqueous phase (above ca. 13 mPa.s) leads to change of the emulsification regime from inertial turbulent to viscous turbulent, while the volume where the dissipation of energy takes place remains almost the same.

References:

1. Tcholakova, S.; Denkov, N. D.; Danner, T. Role of surfactant type and concentration for the mean drop size during emulsification in turbulent flow. *Langmuir* **2004**, *20*, 7444-7458.
2. Tcholakova, S.; Denkov, N. D.; Sidzhakova, D.; Ivanov, I. B.; Campbell, B. Interrelation between drop size and protein adsorption at various emulsification conditions. *Langmuir* **2003**, *19*, 5640-5649.
3. Taisne, L.; Walstra, P.; Cabane, B. Transfer of oil between emulsion droplets. *J. Colloid Interface Sci.* **1996**, *184*, 378.
4. Kolmogoroff, A. N. Drop breakage in turbulent flow. *Compt. Rend. Acad. Sci. URSS*, **1949**, *66*, 825.
5. Hinze, J. O. Fundamentals of the hydrodynamic mechanism of splitting up in dispersion processes. *AIChE Journal* **1955**, *1*, 289.
6. Lagisetty, J. S.; Das, P. K.; Kumar, R.; Gandhi, K. S. Breakage of viscous and non-newtonian drops in stirred dispersions. *Chem. Eng. Sci.* **1986**, *41*, 65.
7. Levich, V. G. *Physicochemical Hydrodynamics*, Prentice Hall, Englewood Cliffs, New Jersey, 1962.
8. Walstra, P.; Smulders, P. Formation of emulsions. In *Proceedings of the 1st World Congress on Emulsions*; Paris, France, 1993.
9. Hinze, J. O. *Turbulence*, McGraw-Hill, New York, 1975.
10. Narsimhan, G.; Goel, P. Drop coalescence during emulsion formation in a high-pressure homogenizer for tetradecane-in-water emulsion stabilized by sodium dodecyl sulfate. *J. Colloid Interface Sci.* **2001**, *238*, 420.